Nuclear Instruments and Methods in Physics Research B 116 (1996) 37–42

ELSEVIER

NIM B
Beam Interactions with Materials & Atoms

Track creation in SiO_2 and $BaFe_{12}O_{19}$ by swift heavy ions: a thermal spike description

M. Toulemonde [a,*], J.M. Costantini [b], Ch. Dufour [c], A. Meftah [d], E. Paumier [a,c], F. Studer [e]

[a] *CIRIL, Laboratoire mixte CEA-CNRS, BP 5133, 14040 Caen Cedex, France*
[b] *CEA-PTN, BP 12, F-91680 Bruyères le Chatel, France*
[c] *LERMAT-ISMRA, URA CNRS 1317, 6 Bd du Maréchal Juin, 14050 Caen Cedex, France*
[d] *GANIL, BP 5027, 14021 Caen Cedex, France*
[e] *CRISMAT-ISMRA, 6 Bd du Maréchal Juin, 14050 Caen Cedex, France*

Abstract

The thermal spike model is used in order to calculate the track radii variation versus electronic stopping power S_e in two radiolysis resistant oxides: SiO_2 quartz and $BaFe_{12}O_{19}$. The mean diffusion length λ of the energy deposited on the electrons is determined by fitting latent track radii versus S_e: 4.0 ± 0.3 and 8.2 ± 1.3 nm respectively for both materials. A decrease in the band gap E_g (12 and 1 eV respectively) means an increase in λ.

1. Introduction

In most of radiolysis resistant insulators a strongly damaged zone is induced along the path of a swift heavy ion by its slowing down in the electronic stopping power regime [1,2]. High resolution electron microscopy [3,4] combined with other physical characterisations [4] made it possible to have a coherent body of experimental results on tracks in several materials [5–8]. However the damage mechanism is unknown. In the 60s the thermal spike model [1,9,10] was superseded by the ionic spike model [2] in order to explain that insulators are sensitive contrary to metallic materials. In the 80s, due to the use of swift heavy ion accelerators, the state of the art has completely changed. Metallic materials whatever they are in an amorphous state [11] or in crystalline one [12–14] can be sensitive to ion beam irradiation in the electronic stopping power regime. A recent detailed development [14,15] of the thermal spike model allows a relatively good description of the observed effects in metals. Concerning the insulators, Sigrist and Balzer [16] have shown that the electronic stopping power threshold of chemical etching of numerous insulators cannot be scaled by the parameters governing the ionic spike model. On the contrary a better correlation appears between the threshold and the thermal conductivity of the irradiated insulators but not with the melting temperature in agreement with the first experimental results [1]. In the same way the electronic sputtering [17,18] was also interpreted on the basis of a thermal process. So it appears that the thermal spike process has to be reconsidered in the case of insulators.

The present paper aims at proposing a first detailed approach of the use of the thermal spike model in order to describe quantitatively the *amorphous track radii induced in crystalline radiolysis resistant insulators* by swift heavy ions. Very recently an analytical version of the thermal spike model was applied to magnetic insulators [19] showing the importance of the melting temperature of the irradiated material contrary to that of Sigrist and Balzer [16]. Moreover it is concluded [19] that the energy density necessary for the formation of the track is lower than the deposited one. However in this model it is difficult to include the track radii determined in SiO_2 quartz [7]. Even with a first numerical solution of the thermal spike model [7,20], only a qualitative description of the latent track radius variation versus electronic stopping power ($-dE/dx = S_e$) was obtained in this material.

In the thermal spike model the energy lost by the slowing down of a heavy ion is given to the target electrons and is then transferred to the lattice through electron–electron and electron–phonon interactions [1,17,21,22]. The effect of those interactions is assumed to be described by only one parameter [7,20]: λ the mean diffusion length of the deposited energy on the electrons. As expected due to this diffusion length, the energy density needed for track formation is lower than the initial one [23,24]. The mechanism of heat transfer from electrons to lattice depends on whether the material is a metal or an insulator [17,20–22]. In metals the heat conduction due to free electrons results in thermalization of hot electrons inside the excited region with cold electrons at the periph-

* Corresponding author.

PII S0168-583X(96)00007-9

ery of this region. In insulators the charges are localized and there are no free electrons outside the excited region. Therefore Baranov et al. [17] proposed the following description: hot electrons excited in the conduction bands behave like hot electrons in metals. The energy dissipation in the electronic system proceeds via the ionization of bound electrons at the periphery of the excited region [22]. The energy spread stops when the electron energy becomes smaller than the ionization one. Therefore λ should increase when the ionization energy decreases. That means that λ should increase when the band gap E_g decreases. Till now such a detailed comparison was not possible because the radial distribution of the initial energy deposition on the electrons was not used directly [23,24].

So the goal of this paper is to apply a new numerical development of the thermal spike model [25] on two insulators, SiO_2 ($E_g = 12$ eV) and $BaFe_{12}O_{19}$ ($E_g = 1$ eV), taking into account the initial radial energy distribution [23]. The λ values are deduced.

2. The thermal spike model in insulators

The thermal spike model is described mathematically by two coupled equations [14,15,21] governing the energy diffusion on the electron and lattice subsystems respectively and their coupling. In a cylindrical geometry the two equations are:

$$C_e \frac{\partial T_e}{\partial t} = \nabla(K_e \nabla T_e) - g(T_e - T) + B(r, t),$$

$$\rho C(T) \frac{\partial T}{\partial t} = \nabla(K(T) \nabla T) + g(T_e - T),$$

where K_e is the electron thermal conductivity, C_e the electron specific heat, g the electron–phonon coupling constant [4], ρ, $C(T)$ and $K(T)$ the specific mass, the specific heat and thermal conductivity of the lattice respectively, and T_e and T the electronic and lattice temperature respectively. t and r are the variables of time and space in cylindrical geometry. The electronic thermal diffusivity is defined by the relation $D_e = K_e / C_e$.

The initial spatial energy distribution $D(r)$ is determined by Waligorski et al. [23]. It depends on the beam energy. It is assumed as previously [15] that the energy deposition time τ is equal to 10^{-15}s, time necessary to slow down the delta-rays electrons [24]. In the present case we assume that $B(r, t) = AD(r)\alpha e^{-\alpha t}$ where $\alpha = 1/\tau$ and A is chosen so that

$$\int_{t=0}^{\infty} \int_{r=0}^{r=r_m} B(r, t) 2\pi r \, dr \, dt = S_e, \; r_m$$

being the maximum range for electrons projected perpendicularly to the ion path [23]. As previously tested [25] a variation of τ by a factor of 5 has no influence on the results.

Contrary to a metal [14] it is difficult to determine the parameters describing the energy relaxation on the electron subsystem and the energy transfer to the atoms. Following the hypothesis suggested by Baranov et al. [17] we shall consider that hot electrons (the electronic temperature is equal or larger than the Fermi temperature) in the conduction band of an insulator will behave like hot electrons in a metal. Consequently the hot electron specific heat [26] and the hot electron diffusivity [27] can be considered as constant: $C_e \sim 1$ J cm^{-3} K^{-1} and $D_e \sim 2$ cm^2 s^{-1}. So in order to be able to consider the precise spatial time evolu-

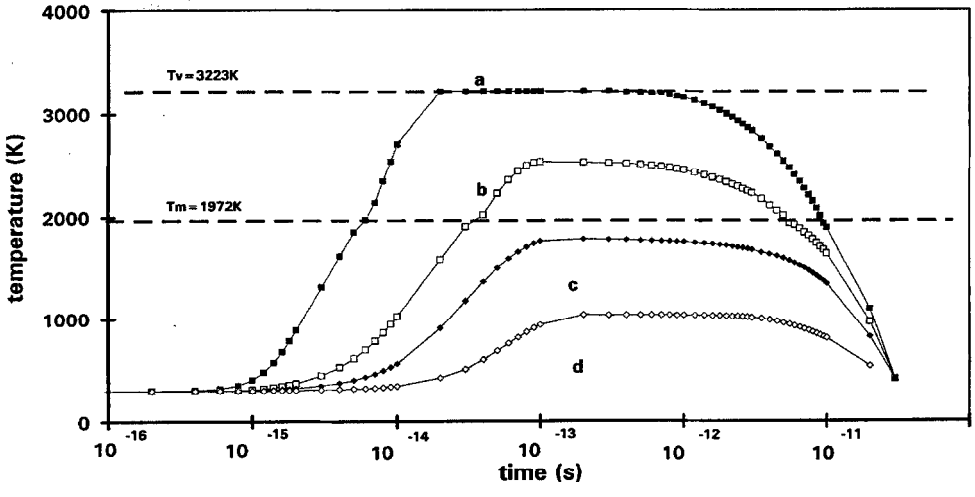

Fig. 1. For $\lambda = 4$ nm evolution of the lattice temperature versus time at a distance of 1 (a), 3 (b), 4.5 (c) and 8 (d) nm from the ion path in SiO_2. The krypton beam energy was 3.4 MeV/amu corresponding to a $S_e = 12$ keV/nm. The sample was at 300 K. T_m and T_v correspond to the melting and vaporization temperature respectively.

tion of the deposited energy on the electron, a numerical solution of the first equation is used [25].

The electron–phonon coupling constant g is linked to the electron–phonon interaction mean time τ_a by the relation $\tau_a = C_e/g$ [21] and to the mean diffusion length λ of the deposited energy, by the relation $\lambda^2 = D_e\tau_a$. In the present calculation, λ will be considered as the free parameter: it is the unknown parameter directly related to the electron–phonon coupling constant since D_e and C_e are constant.

A numerical solution of the second equation is also performed in order to take into account the temperature dependence of the lattice thermodynamical parameters as well as the solid–liquid phase change. All those parameters are given in Ref. [7] for SiO_2 quartz and in Table 1 for $BaFe_{12}O_{19}$ [28].

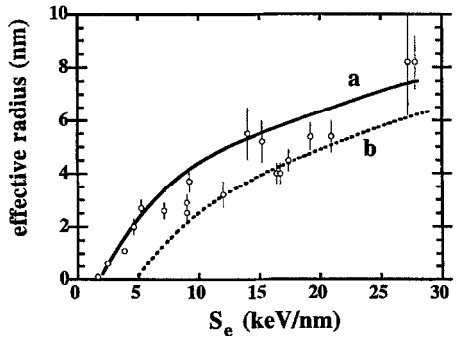

Fig. 2. Effective radii of track versus S_e for SiO_2 quartz. The circles correspond to the experimental points. The line corresponds to two specific calculations using the thermal spike model: (a) $\lambda = 3.7$ nm and the beam energy 0.2 MeV/amu; (b) $\lambda = 4.3$ nm and the beam energy 5 MeV/amu.

3. Calculations

3.1. SiO_2 quartz and $BaFe_{12}O_{19}$

The results of the calculation for SiO_2 quartz [7] are given in Fig. 1 where the lattice temperature evolution is reported versus the time at different distances from the ion axis. For a time less than 10^{-13} s the "temperature" characterises the energy which is given to the atoms. In the case presented on Fig. 1 the track radius is around 4.0 nm assuming that it results from the quenching of the molten phase and that no recrystallisation occurs at the solid–liquid interface due to the very high quenching rate (10^{14} K/s). The calculation is performed for each experimental point reported in Ref. [7] for continuous tracks (i.e. with an effective experimental radius larger than 2 nm [6]). For each case the λ value is extracted taking into account the experimental determination of the track radius. A mean value of $\lambda = 4.0 \pm 0.3$ nm is deduced and the radius evolution of the track versus S_e is reported in Fig. 2 for the extreme values of λ and beam energy. Contrary to the previous calculation [7], the present theoretical determination of the track radii closely follows the overall evolution of R_e versus S_e. The λ value is twice as small as the previous one [7] obtained with a Gaussian approximation of the initial spatial energy distribution. This result clearly shows the importance of a precise description of the initial spatial energy deposition shape. It also shows that the simplified version of the thermal spike model [7] overestimates the induced temperature increase.

Table 1
Macroscopic thermodynamical parameters for $BaFe_{12}O_{19}$

Thermal conductivity [W/K cm]	0.07 (solid) Ref. [28]
	0.035 (liquid) Ref. [28]
Specific heat [J/g K]	0.76 (Dulong–Petit law) Ref. [26]
Melting temperature [K]	1741
Latent heat of fusion [J/g]	240 Ref. [19]
Volumic mass [g/cm^3]	5.17 (solid)
	4.90 (liquid)

Recently [6] it has been shown that the damage cross section in yttrium iron garnet $Y_3Fe_5O_{12}$ is higher at low ion velocity than at high ion velocity for the same value of dE/dx. Katz and Kobetich [29] have calculated the spatial energy distribution of the energy deposited on the electrons: this distribution is broader at high velocity than at low velocity. That means that for the same value of dE/dx the local deposited energy per unit volume is larger at low velocity than at high velocity. Waligorski, Hamm and Katz [23] have proposed an analytical formula to describe the radial profile of the spatial energy deposition deduced from a fit of Monte Carlo results. Using this formula, a cylinder with a radius R in which 65% of the energy is deposited, is defined [6]. The mean energy density E_d can be defined in this cylinder for a given specific value of S_e and beam energy:

$$E_d = 0.65\ S_e/N_a\pi R^2,$$

where N_a is the atomic density. The effective radius R_e of track is plotted versus E_d in Fig. 3 for different ranges of beam energy. The results of the calculation are also reported for $\lambda = 4$ nm at different beam energy ranges showing a very good agreement.

The same calculations are performed for $BaFe_{12}O_{19}$ (Figs. 4 and 5) and a mean value of $\lambda = 8.2 \pm 1.3$ nm is extracted by fitting all the experimental results [5]. There is also a very good agreement between experimental results and the theoretical calculation of the track radii taking the extreme values of λ and beam energy.

It can be seen by comparison of the results presented in Figs. 1 and 4 that the maximum temperature reached in the SiO_2 quartz is larger than in $BaFe_{12}O_{19}$. It results from the fact that λ is lower in SiO_2 quartz than in $BaFe_{12}O_{19}$.

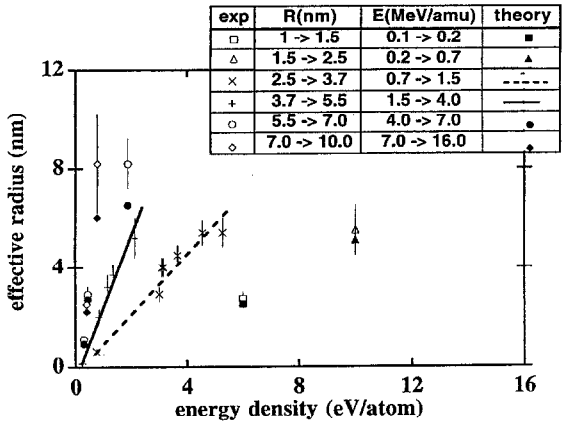

Fig. 3. Effective radii of track versus the deposited energy density in SiO_2 quartz.

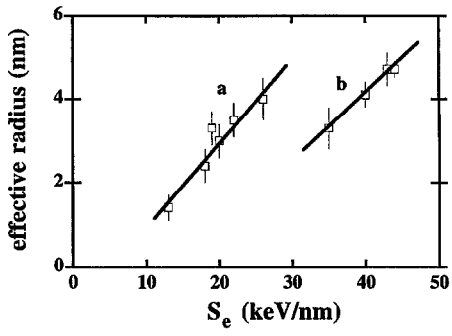

Fig. 5. Effective radii of track versus S_e for $BaFe_{12}O_{19}$. The circles correspond to the experimental points. The lines correspond to two specific calculations using the thermal spike model: (a) $\lambda = 6.9$ nm and the beam energy 7 MeV/amu; (b) $\lambda = 9.5$ nm and the beam energy 23 MeV/amu.

3.2. Discussion of the input parameters

The parameter λ, the mean diffusion length of the deposited energy, is the free parameter. It is twice as large for $BaFe_{12}O_{19}$ as for SiO_2. The question is to know whether this relative evolution depends on the initial values of D_e and C_e. The results of the calculation are identical for different D_e values provided that $D_e\ \tau_a$ product leads to the same value of λ for D_e ranging between 1 and 20 $cm^2\ s^{-1}$. Hot electron specific heat depends on the number of excited electrons [26]. For SiO_2 quartz C_e can vary between 0.5 $J\ cm^{-3}\ K^{-1}$, if we assume that the number of excited electrons corresponds to the number of valence electrons, and 1.6 $J\ cm^{-3}\ K^{-1}$ if there is one excited electron per atom. Such a variation of C_e induces a $\pm 15\%$ variation of λ. For $BaFe_{12}O_{19}$ the same range of C_e variation leads to a $\pm 10\%$ variation of λ. As λ does not depend significantly on the values of the electronic parameters, it should be linked to other physical parameters of the irradiated materials.

4. Discussion

Taking into account all the hypotheses that we have made, it is very encouraging to get a very good agreement between experiment and the modelisation for the effective radius evolution of tracks versus S_e using only one fitting parameter: the electron–phonon mean free path.

For SiO_2, the knowledge of λ allows the determination of τ_a, the mean electron–phonon interaction time using the relation $\lambda^2 = D_e\ \tau_a$. With a realistic value of D_e (1 to 2

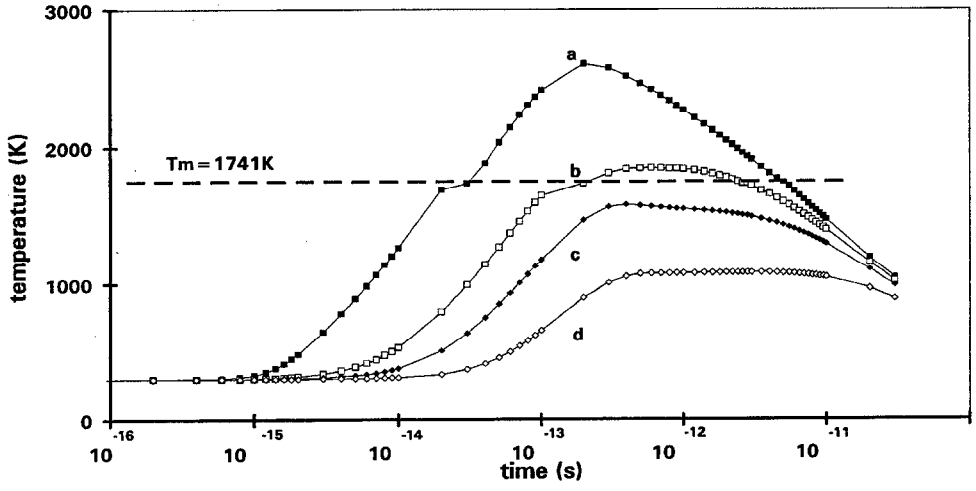

Fig. 4. For $\lambda = 8.2$ nm evolution of the lattice temperature versus time at distances of 1 (a), 3 (b), 4 (c) and 7.5 (d) nm from the ion path in $BaFe_{12}O_{19}$. The xenon beam energy was 7 MeV/amu corresponding to $S_e = 26$ keV/nm. The sample was at 300 K. T_m is the melting temperature.

cm^2/s for hot electrons [27]) τ_a varies between 160 and 80 fs. Such a determination is possible since the ion energy is deposited on the electrons in a small cylinder and in a time less than 10 fs [24], i.e. one order of magnitude less than τ_a [7,23]. This value of τ_a is of the same order of magnitude as the one deduced from fs laser experiments (150 fs [30]).

The λ evolution between the two materials is also in agreement with the description made by Katin et al. [22] and Baranov et al. [17]: λ in solid insulators should increase when the ionization energy of the valence electrons (band gap energy) decreases, going from 12 eV for SiO_2 to 1 eV for $BaFe_{12}O_{19}$. The extrapolation of such description is not straightforward. Is it linear? Several other materials have to be irradiated in order to determine the λ evolution versus the band gap energy.

Can we extend such a description to non-amorphizable materials like Al_2O_3 and MgO [31,32] and for radiolysis sensitive materials like the alkali-halides [33]? In Al_2O_3 and MgO, the free carriers lifetime, deduced from fs laser irradiation [31], is two orders of magnitude larger than in SiO_2 quartz. This implies that λ should increase by one order of magnitude. Using such a scaling in the present calculation of the thermal spike Al_2O_3 and MgO will be insensitive to S_e in contradiction with the results of irradiation performed with swift heavy ions [32]. Such a contradiction shows the present limits of comparison between heavy ions and fs laser irradiations in insulators. Higher deposited energy density is needed with fs laser irradiations to make reliable comparisons. In the case of alkali-halides the conclusion made previously [33] has to be checked using the present numerical solution of the thermal spike modelisation.

5. Conclusion

In conclusion, by using the thermal spike model in order to describe the track radii evolution in two oxide materials (SiO_2 quartz, $BaFe_{12}O_{19}$), we have correlated the mean diffusion length λ of the deposited energy to the width of the band gap. Such a conclusion has to be checked in the case of other amorphisable radiolysis resistant insulators in order to know whether such a description can be extended. Other questions are still open linked to non-amorphizable radiolysis resistant materials and to radiolysis sensitive ones.

References

[1] L.T. Chadderton and I.McC. Torrens, Fission damage in crystals (Methuen, 1969) pp. 113 and 190.

[2] R.L. Fleisher, P.B. Price and R.M. Walker, Nuclear Tracks in Solids and its Applications (Univ. of California Press, Berkeley, CA, 1975).

[3] C. Houpert, F. Studer, D. Groult and M. Toulemonde, Nucl. Instr. and Meth. B 39 (1989) 720.

[4] M. Toulemonde and F. Studer, Philos. Mag. A 58 (1988) 799.

[5] F. Studer, C. Houpert, H. Pascard, R. Spohr, J. Vetter, Y.F. Jin and M. Toulemonde, Radiat. Eff. Def. Solids 116 (1991) 59.

[6] A. Meftah, F. Brisard, J.M. Costantini, M. Hage-Ali, J.P. Stoquert, F. Studer and M. Toulemonde, Phys. Rev. B 48 (1993) 920.

[7] A. Meftah, F. Brisard, J.M. Costantini, E. Dooryhee, M. Hage-Ali, M. Hervieu, J.P. Stoquert, F. Studer and M. Toulemonde, Phys. Rev. B 49 (1994) 12457.

[8] M. Toulemonde, F. Studer and S. Bouffard, Nucl. Instr. and Meth. B 91 (1994) 108.

[9] G. Bonfiglioli, A. Ferro and A. Mojoni, J. Appl. Phys. 32 (1961) 2499.

[10] H. Blank, Phys. Status Solidi 10 (1972) 465.

[11] S. Klaumünzer and G. Schumacher, Phys. Rev. Lett. 51 (1987) 1987.

[12] A. Dunlop, D. Lesueur, J. Morillo, J. Dural, R. Spohr and J. Vetter, CR Acad. Sci. 1277 (1989) 309.

[13] A. Audouard, E. Balanzat, S. Bouffard, J.C. Jousset, A. Chamberod, A. Dunlop, D. Lesueur, G. Fuchs, R. Spohr, J. Vetter and L. Thomé, Phys. Rev. Lett. 65 (1990) 875.

[14] C. Dufour, A. Audouard, F. Beuneu, J. Dural, J.P. Girard, A. Hairie, M. Levalois, E. Paumier and M. Toulemonde, J. Phys. Condens. Matter 5 (1993) 4573.

[15] Z.G. Wang, Ch. Dufour, E. Paumier and M. Toulemonde, J. Phys. Condens. Matter 6 (1994) 6733 and 7 (1995) 2525.

[16] A. Sigrist and R. Balzer, Helv. Phys. Acta 50 (1977) 49 and Radiat. Eff. 34 (1977) 75.

[17] I.A. Baranov, Yu V. Martinenko, S.O. Tsepelevitch and Yu N. Yavlinskii, Sov. Phys. Usp. 31 (1988) 1015.

[18] R.E. Johnson, B.U.R. Sundquist, A. Hedin and D. Fenyö, Phys. Rev. B 46 (1992) 14362.

[19] G. Szenes, Phys. Rev. B 51 (1995) 8026.

[20] M. Toulemonde, C. Dufour and E. Paumier, Phys. Rev. B 46 (1992) 14362.

[21] I.M. Lifshitz, M.I. Kaganov and L.V. Tanatarov, J. Nucl. Energy A 12 (1960) 69.

[22] V.V. Katin, Yu V. Martinenko and Yu N. Yavlinskii, Sov. Techn. Phys. Lett. 13 (1987) 276.

[23] M.P.R. Waligorski, R.N. Hamm and R. Katz, Nucl. Tracks Radiat. Meas. 11 (1986) 309.

[24] B. Gervais and S. Bouffard, Nucl. Instr. and Meth. B 88 (1994) 355.

[25] C. Dufour, B. Lesellier De Chezelles, V. Delignon, M. Toulemonde and E. Paumier, Modifications induced by irradiation in glasses, ed. P. Mazzoldi (Elsevier, North-Holland, 1992) p. 61.

[26] N.W. Ashcroft and N.D. Mermin, Solid State Physics (Holt, Reinhart and Winston, New York, 1976).

[27] Yu.V. Martynenko and Yu.N. Yavlinskii, Sov. Phys. Dokl. 28 (1983) 391.

[28] A. Neda, Studia Univ. Bales-Bolyai Physica 1 (1970) 10.

[29] R. Katz and E.J. Kobetich, Phys. Rev. 186 (1969) 344.
[30] P. Audebert, Ph. Daguzan, A. Dos Santos, J.C. Gauthier, J.P. Geindre, S. Guizard, G. Hamoniaux, K. Krastev, P. Martin, J. Petite and A. Antonetti, Phys. Rev. Lett. 73 (1994) 1990.
[31] S. Guizard, P. Martin, Ph. Daguzan, J. Petite, P. Audebert, J.P. Geindre, A. Dos Santos and A. Antonetti, Europhys. Lett. 29 (1995) 401.
[32] B. Canut, S.M.M. Ramos, P. Thevenard, N. Moncoffre, A. Benyagoub, J. Marest, A. Meftah, M. Toulemonde and F. Studer, Nucl. Instr. and Meth. B 80/81 (1993) 1114.
[33] L. Protin, E. Balanzat, A. Cassimi, E. Dooryhée, J.L. Doualan, E. Paumier and M. Toulemonde, Radiat. Eff. Def. Solids 136 (1995) 287.